Journal of Biomechanics 95 (2019) 109329

Contents lists available at ScienceDirect

Journal of Biomechanics

journal homepage: www.elsevier.com/locate/jbiomech
www.JBiomech.com

Short communication

Can a reduction approach predict reliable joint contact and musculo-tendon forces?

Raphael Dumas [a,*], Arnaud Barré [b], Florent Moissenet [c], Rachid Aissaoui [d,e]

[a] Univ Lyon, Université Claude Bernard Lyon 1, IFSTTAR, LBMC UMR_T9406, LBMC, F69622 Lyon, France
[b] Moveck Solution Inc., Québec, Canada
[c] Willy Taillard Laboratory of Kinesiology, University Geneva Hospitals and Geneva University, Geneva, Switzerland
[d] Laboratoire de Recherche en Imagerie et Orthopédie, Centre de Recherche du CHUM, Canada
[e] Département de génie des systèmes, École de Technologie Supérieure, Montréal, Canada

ARTICLE INFO

Article history:
Accepted 30 August 2019

Keywords:
Musculoskeletal model
Joint loadings
Lower limb
Gait
Instrumented prosthesis
Validation

ABSTRACT

Musculoskeletal models generally solve the muscular redundancy by numerical optimisation. They have been extensively validated using instrumented implants. Conversely, a reduction approach considers only one flexor or extensor muscle group at the time to equilibrate the inter-segmental joint moment. It is not clear if such models can still predict reliable joint contact and musculo-tendon forces during gait.

Tibiofemoral contact force and gastrocnemii, quadriceps, and hamstrings musculo-tendon forces were estimated using a reduction approach for five subjects walking with an instrumented prosthesis. The errors in the proximal-distal tibiofemoral contact force fell in the range (0.3–0.9 body weight) reported in the literature for musculoskeletal models using numerical optimisation. The musculo-tendon forces were in agreement with the EMG envelops and appeared comparable to the ones reported in the literature with generic musculoskeletal models.

Although evident simplifications and limitations, it seems that the reduction approach can provided quite reliable results. It can be a useful pedagogical tool in biomechanics, e.g. to illustrate the theoretical differences between inter-segmental and contact forces, and can provide a first estimate of the joint loadings in subjects with limited musculoskeletal deformities and neurological disorders.

1. Introduction

In parallel to the development of musculoskeletal models which solve the muscular redundancy by numerical optimisation (Damsgaard et al., 2006; Delp et al., 2007), more simple models are based on a reduction approach, e.g. (DeVita and Hortobagyi, 2001; Johnson et al., 1981; Paul, 1999; Smidt, 1973). The principle is to consider only one flexor or extensor muscle group at the time to equilibrate the inter-segmental joint moment. Such reduction approach is currently used in the biomechanical community for the estimation of contact forces in osteoarthritic and ligament-reconstructed patients, and healthy volunteers during walking and running (Bowersock et al., 2017; Esculier et al., 2017; Kernozek et al., 2017; Messier et al., 2013; Sinclair and Bottoms, 2019; Willy et al., 2016). Thanks to its numerical efficiency, the reduction approach allows for very large study samples, e.g. up to 418 subjects in the study of Johnson et al. (1981) and 372 in the study of Messier et al. (2013).

While musculoskeletal models using numerical optimisation have been extensively validated using instrumented implants, e.g. (Heller et al., 2001; Kinney et al., 2013), the reduction approach has been hardly evaluated. Only a preliminary validation (errors on proximal-distal tibiofemoral contact force peaks below 10% during gait) has been reported using the data of one subject with an instrumented prosthesis (Messier et al., 2013). This reported level of error, below 10%, compares favourably with the errors obtained with numerical optimisation (Moissenet et al., 2017). However, this preliminary validation was performed on one subject and was limited to peak values of the proximal-distal tibiofemoral contact force. Thus, the objective of this study is to evaluate both the tibiofemoral contact force and the musculo-tendon forces estimated by a reduction approach (DeVita and Hortobagyi, 2001) to confirm if such an approach can predict reliable joint contact and musculo-tendon forces during the gait of different subjects. This is done using the reference data provided by the *Grand Challenge*

* Corresponding author at: IFSTTAR, LBMC, UMR_T9406, Bron, France.
E-mail address: raphael.dumas@ifsttar.fr (R. Dumas).

https://doi.org/10.1016/j.jbiomech.2019.109329
0021-9290/

Competition to Predict In Vivo Knee Loads (Fregly et al., 2012) and the *CAMS-Knee* (Taylor et al., 2017) datasets.

2. Material and methods

2.1. Literature datasets

Five gait cycles of four subjects with an instrumented posterior cruciate ligament retaining prosthesis (*Grand Challenge* competitions #1, #2, #3, #5 (Fregly et al., 2012)) and three gait cycles of one subject with an instrumented ultra-congruent prosthesis (*CAMS-Knee* sample K8L (Taylor et al., 2017)) were analysed.

2.2. Computation method and model

The ankle, knee, and hip flexion-extension angles and moments were computed by a multi-body kinematics optimisation with, respectively, universal, hinge and spherical joints (Duprey et al., 2010) followed by an inverse dynamics computation using wrenches and quaternions (Dumas et al., 2004). Then, tibiofemoral contact force and gastrocnemii, quadriceps, and hamstrings musculo-tendon forces (Fig. 1) were estimated using the reduction approach proposed by DeVita and Hortobagyi (2001). The reader can refer to this original article for a 2D illustration of the knee joint and a scalar formulation of the problem. This formulation can be summarised in the following invertible system:

$$\begin{pmatrix} \mathbf{F}_2 \cdot \mathbf{X}_2 \\ \mathbf{F}_2 \cdot \mathbf{Y}_2 \\ r_1(\mathbf{M}_1 \cdot \mathbf{Z}_2) \\ \mathbf{M}_2 \cdot \mathbf{Z}_3 \\ r_3(\mathbf{M}_3 \cdot \mathbf{Z}_4) \end{pmatrix} = \begin{bmatrix} 1 & 0 & \mathbf{u}^1 \cdot \mathbf{X}_2 & \mathbf{u}^2 \cdot \mathbf{X}_2 & \mathbf{u}^3 \cdot \mathbf{X}_2 \\ 0 & 1 & \mathbf{u}^1 \cdot \mathbf{Y}_2 & \mathbf{u}^2 \cdot \mathbf{Y}_2 & \mathbf{u}^3 \cdot \mathbf{Y}_2 \\ 0 & 0 & L_1^1 & 0 & 0 \\ 0 & 0 & L_2^1 & L_2^2 & L_2^3 \\ 0 & 0 & 0 & 0 & L_3^3 \end{bmatrix} \begin{pmatrix} \mathbf{R}_2 \cdot \mathbf{X}_2 \\ \mathbf{R}_2 \cdot \mathbf{Y}_2 \\ f^1 \\ f^2 \\ f^3 \end{pmatrix} \quad (1)$$

with $\mathbf{X}_i$, $\mathbf{Y}_i$, and $\mathbf{Z}_i$ the axes of the segment coordinate system (i = 1, 2, 3, and 4 for foot, shank, thigh, and pelvis segments (Wu et al., 2002), respectively), $\mathbf{F}_i$, $\mathbf{M}_i$ and $\mathbf{R}_i$ the inter-segmental forces and moments and contact forces applied at the origin of the segment coordinate system and standing for the action of the proximal segment on the distal segment (i.e. thigh on shank for i = 2), L_i^j, $\mathbf{u}^j$, and f^j the muscle group's lever arms, line of action orientations, and musculo-tendon forces (j = 1, 2, and 3 for gastrocnemii, quadriceps, and hamstrings, respectively), and r_i the ratios of joint moments accounted for. Not all of the components of the inter-segmental forces and moments and contact forces are included in the computation and the projection of these vectors on the relevant segment axes are obtained with a dot product (.).

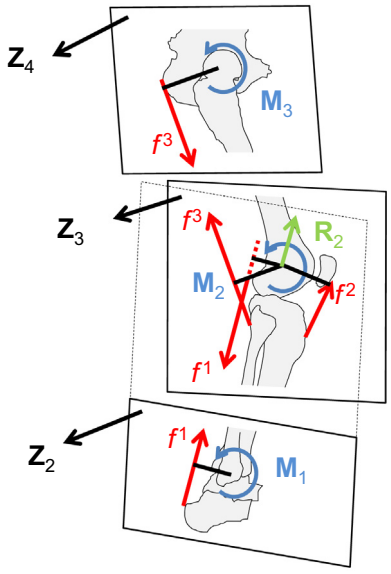

Fig. 1. Principle of the reduction approach: the tibiofemoral contact force (in green) and the forces in the gastrocnemii, quadriceps, and hamstrings (in red) are estimated from the ankle, knee and hip flexion-extension moments (in blue) knowing each muscle group's lever arm and line of action orientation. (For interpretation of the references to colour in this figure legend, the reader is referred to the web version of this article.)

In the present study, the muscle groups lever arms and line of action orientations (L_i^j and $\mathbf{u}^j$) were defined by polynomial functions of the ankle, knee and hip joint angles (Appendix). No scaling of this muscle geometry to the subject anthropometry was performed. Two constant ratios, respectively for the contribution of the gastrocnemii to the ankle flexion-extension moment and for the contribution of the hamstrings to the hip flexion-extension moment, were set (Messier et al., 2011):

$$r_1 = 0 \text{ if } \mathbf{M}_1 \cdot \mathbf{Z}_2 > 0 (\text{flexion}) \text{ and } r_1 = 0.319 \text{ if } \mathbf{M}_1 \cdot \mathbf{Z}_2 < 0 (\text{extension}) \quad (2)$$

$$r_3 = 0 \text{ if } \mathbf{M}_3 \cdot \mathbf{Z}_4 > 0 (\text{flexion}) \text{ and } r_3 = 0.63 \mathbf{M}_3 \cdot \mathbf{Z}_4 < 0 (\text{extension}) \quad (3)$$

The contribution of the gastrocnemii to the ankle joint moment, either 0 or a constant ratio, is based, respectively, on the mechanical action of this extensor muscle group and on a proportion of the cross sectional areas of the posterior calf muscles. The contribution of the hamstrings to the hip joint moment is also based on the mechanical action of this extensor muscle group and on a proportion of both lever arms and cross sectional areas of the posterior thigh muscles (DeVita and Hortobagyi, 2001).

2.3. Validation

With the ultra-congruent prosthesis, the anterior-posterior component of the tibiofemoral contact force ($\mathbf{R}_2.\mathbf{X}_2$) was quantitatively validated by computing the root mean square error (RMSE), the error of force peak(s), and the coefficient of determination (R^2) between the estimated and the experimentally measured forces This component of the tibiofemoral contact force is available in the *Grand Challenge* dataset (Fregly et al., 2012) but the force in the posterior cruciate ligament (i.e. neither computed nor measured) make comparisons difficult. The proximal-distal component of the tibiofemoral contact force ($\mathbf{R}_2.\mathbf{Y}_2$) was validated with all prostheses.

Musculo-tendon forces (f^1, f^2, f^3) were semi-quantitatively validated by computing their concordance coefficient (C) (Giroux et al., 2013) with the experimentally measured surface EMG envelops of gastrocnemius medialis and lateralis, vastus medialis and lateralis, rectus femoris, semimembranosus and biceps femoris caput longum. This concordance coefficient quantifies the agreement between active/inactive states derived from the estimated forces and the measured EMG envelops during seven different phases of the gait cycle (Perry and Burnfield, 2010). In each phase, if the mean is above 10% of the maximal force over the gait cycle (20% of the maximal EMG), the muscle state is active, otherwise inactive.

3. Results

The average RMSEs between the estimated and the measured anterior-posterior tibiofemoral contact forces ($\mathbf{R}_2.\mathbf{X}_2$) were 0.13 times the body weight (BW) and poor correlations were found

between them (Table 1, Fig. 2). The mean error on the peak force was 0.04 BW.

The average RMSEs between the estimated and the measured proximal-distal tibiofemoral contact forces ($\mathbf{R}_2.\mathbf{Y}_2$) were between 0.39 and 0.63 BW and good to strong correlations were found between them. Mean errors were between 0.06 and 1.06 BW on the first peak of contact and between 0.37 and 1.10 BW on the second peak.

The average concordance coefficients (C) between the estimated musculo-tendon forces of the three muscle groups and the corresponding measured individual muscle EMG envelops were between 63 and 72%. Looking into details at the curve patterns (Fig. 2), it appeared that the gastrocnemii musculo-tendon forces (f^1) were mainly consistent with the measured EMG envelops at terminal stance, pre-swing and terminal swing. The quadriceps musculo-tendon forces (f^2) were mainly consistent with the measured EMG envelops at loading response and midstance. The hamstrings musculo-tendon forces (f^3) were mainly consistent with the measured EMG envelops at loading response, initial swing and terminal swing.

4. Discussion

The objective of this study was to evaluate the forces estimated by a reduction approach. Even though a preliminary validation has been reported (Messier et al., 2013) and an equivalence between a reduction approach and a musculoskeletal model using numerical optimisation has been shown for the force in the Achilles tendon (Kernozek et al., 2017), such encouraging results were not expected. These results demonstrate that the reduction approach was able to capture the essential features that govern the tibiofemoral contact forces during gait: the main influential muscles, their lever arms and lines of actions. The patterns of all the force curves, except for the anterior-posterior tibiofemoral contact force, were generally matching *in vivo* measurements with correlation (R^2) between 0.71 and 0.92 and concordance (C) between 63 and 72%. This is the level of concordance already reported for more comprehensive muscle geometries (Giroux et al., 2013). The errors in the proximal-distal tibiofemoral contact force fell in the range of RMSEs (0.3–0.9 BW) reported in the literature with generic musculoskeletal models (Moissenet et al., 2017). As for the RMSEs on the

Table 1
Mean and standard deviation of the root mean square errors (RMSE), peak errors, and the coefficients of determination (R^2) between the estimated and the experimentally measured contact forces, and of the concordance coefficients (C) between the estimated musculo-tendon forces the experimentally measured EMG envelops.

		GC #1	GC #2	GC #3	GC #5	CAMS-Knee sample
Anterior-posterior contact force	RMSE (in BW)					0.13 (0.03)
	R^2					0.21 (0.16)
	Peak error (in BW)					0.04 (0.02)
Proximal-distal contact force	RMSE (in BW)	0.63 (0.08)	0.61 (0.16)	0.42 (0.07)	0.49 (0.09)	0.39 (0.02)
	R^2	0.72 (0.06)	0.71 (0.14)	0.77 (0.06)	0.85 (0.05)	0.91 (0.02)
	1st peak error (in BW)	0.94 (0.15)	1.06 (0.25)	0.38 (0.10)	0.18 (0.14)	0.06 (0.06)
	2nd peak error (in BW)	0.53 (0.16)	0.38 (0.33)	0.42 (0.07)	1.10 (0.23)	0.37 (0.09)
Musculo-tendon forces	C (in %)	66 (2)	72 (4)	68 (4)	63 (4)	67 (7)

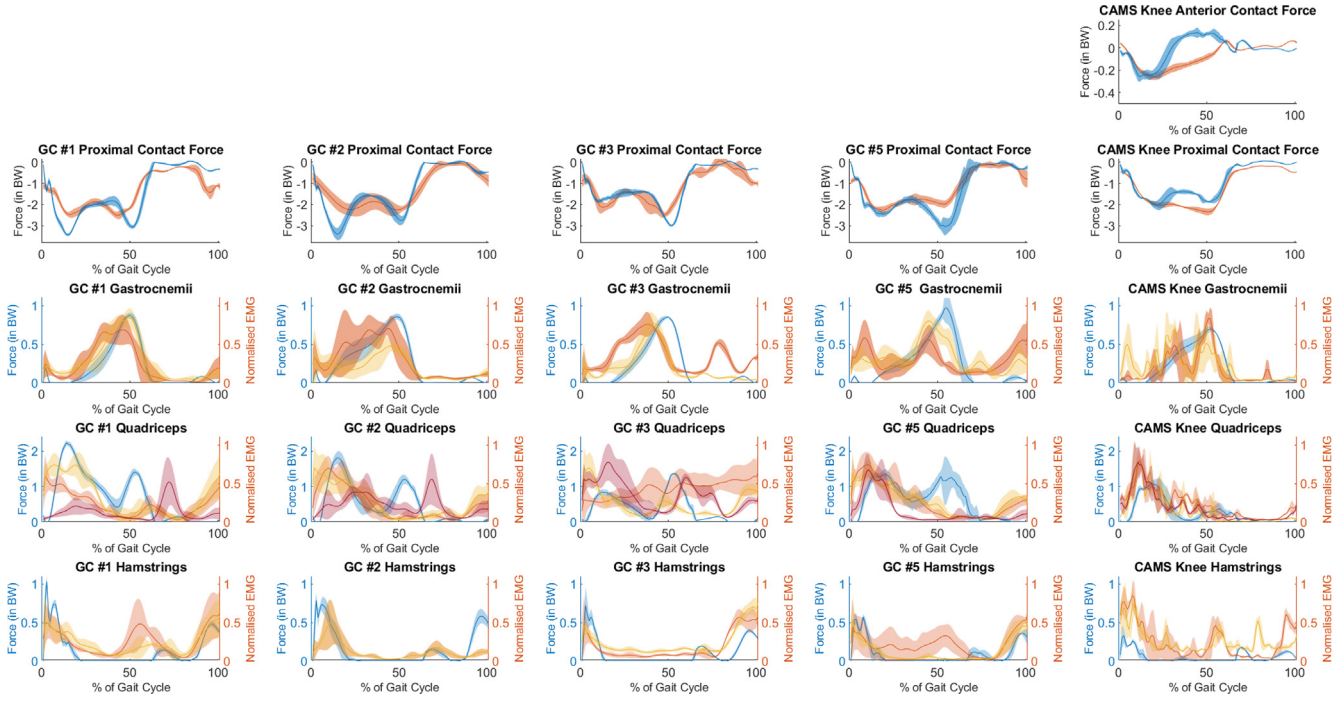

Fig. 2. Mean and standard deviation (shaded area) of the estimated forces (in blue) compared to experimentally measured contact forces and EMG envelops (individual muscle in orange and red) normalised on 100% of gait cycle. Estimated and measured forces are in body weight (BW). EMG envelops are normalised by their maximal value over the different gait trials of the subject. For the gastrocnemii, dark and light orange are for the gastrocnemius medialis and gastrocnemius lateralis, respectively. For the quadriceps, dark and light orange and red are for the vastus medialis, vastus lateralis and rectus femoris, respectively. For the hamstrings, dark and light orange are for the semimembranosus and biceps femoris caput longum, respectively. (For interpretation of the references to colour in this figure legend, the reader is referred to the web version of this article.)

force peaks, they range between 0.06 and 1.10 BW and match the typical errors (0.1–1.7 BW) reported with musculoskeletal models using numerical optimisation (DeMers et al., 2014; Knarr and Higginson, 2015; Thelen et al., 2014). Though, errors reaching 1 BW are challenging the accuracy below 10% reported for the reduction approach (Messier et al., 2013) using the dataset of either *Grand Challenge* competition #1, #2 or #3 (this information was not available). The computation of medial and lateral proximal-distal tibiofemoral contact force could have been also considered with the reduction approach (Barrios and Willson, 2016), using the knee adduction-abduction moment ($\mathbf{M}_2 \cdot \mathbf{X}_2$) and fixed positions of the contact points in the frontal plane of the shank. However, this is not specific to the reduction approach. Indeed, the musculoskeletal models using numerical optimisation generally proceed the same way, e.g. (Winby et al., 2009). Moreover, the patterns and amplitudes of the musculo-tendon forces, especially for the gastrocnemii and hamstrings groups, match the ones reported in the literature with generic musculoskeletal models (Trinler et al., 2018). The comparison is more problematic for the quadriceps because more complex musculoskeletal models differentiate between vastii and rectus femoris. Still, when superimposing the two forces synthetized by Trinler et al. (2018), the pattern and amplitude of the quadriceps musculo-tendon forces obtained with the reduction approach seem in agreement with the ones reported in the literature.

The fact that muscles were grouped in the reduction approach is one of the well-known limitations (Messier et al., 2011). Other evident limitations are the restriction to flexion-extension moments, the simplified lever arms and orientation of the lines of action (depending on one joint angle only), the assumption of no co-contraction at the ankle and hip joints, the absence of ligaments. In spite of these major simplifications, the reduction approach provided quite reliable results in the present validation study which remains, however, limited to five subjects belonging to a marginal category of the population (i.e. elderly, total knee prosthesis) and performing one motor task (i.e. level walking). For the anterior-posterior tibiofemoral contact force, the validation is limited to one subject out the five and the pattern of the force is not reproduced. This component of the contact force should be therefore interpreted with caution. The generalisation of the results to other motor tasks, especially involving higher ankle, knee, and hip flexion-extension angles is also questionable.

Its simplicity makes the reduction approach a useful pedagogical tool in biomechanics, typically to illustrate and make understand the theoretical differences between inter-segmental force and contact force ($\mathbf{F}_2$ vs. $\mathbf{R}_2$) as well as the contribution of each muscle group to the contact force at the knee level. That is, $\mathbf{F}_2 - \left(f^1\mathbf{u}^1 + f^2\mathbf{u}^1 + f^3\mathbf{u}^3\right) = \mathbf{R}_2$ while the muscle forces derive from the inter-segmental moments (i.e. last lines of Eq. (1)). On the proximal-distal axis, $\mathbf{u}^j \cdot \mathbf{Y}_2 > 0$ (j = 1,2,3). The inter-segmental forces applied on the shank ($\mathbf{F}_2 \cdot \mathbf{Y}_2 < 0$) that remains close to one BW in amplitude sums up with all muscle forces and yields a compressive contact force ($\mathbf{R}_2 \cdot \mathbf{Y}_2 < 0$) reaching 3 BW. On the anterior-posterior axis, $\mathbf{u}^1 \cdot \mathbf{X}_2 > 0$ (i.e. gastroctnemii), $\mathbf{u}^2 \cdot \mathbf{X}_2 > 0$ (i.e. quadriceps), but $\mathbf{u}^3 \cdot \mathbf{X}_2 < 0$ (i.e. hamstrings) so that co-contraction at the knee has the potential to reduce the shear force ($\mathbf{R}_2 \cdot \mathbf{X}_2$). It is in this pedagogical perspective that the reduction approach proposed by DeVita and Hortobagyi (2001) is preferentially presented as an invertible system in the present study and that all model parameters are given in Appendix. The reduction approach has been also presented following the ISB convention (Wu et al., 2002) for the segment axes and joint angles. Yet, its simplicity also prevents from extensive personalisation and adaption and the application of the reduction approach shall be limited to subjects with minimal musculoskeletal deformities and neurological disorders. Subjects with a total knee prosthesis like the ones analysed in this validation study are expected to fall in this category. Similarly, the application of the reduction approach to osteoarthritic (Messier et al., 2013) and ligament-reconstructed patients (Bowersock et al., 2017) seems appropriate and allows for very large study samples thanks to its numerical efficiency.

The extension of the reduction approach to compute the ankle contact force is possible. This would require to define the lever arms and lines of action of the flexor muscle group to compute the corresponding muscle force when $\mathbf{M}_1 \cdot \mathbf{Z}_2 > 0$. This would also require to define the lever arms and lines of action of the soleus, its contribution to the ankle extension moment being 0.681. Yet, the validation of the ankle contact force is currently not possible because no ankle instrumented prosthesis exist. On the contrary, validation of the hip contact force is widely held, e.g. (Heller et al., 2001) but the extension of the reduction approach is more problematic due to a higher muscle redundancy and a higher number of degrees of freedom to equilibrate.

Declaration of Competing Interest

The authors do not have any financial or personal relationships with other people or organisations that would have inappropriately influenced this study.

Acknowledgments

The authors would like to thank Paul DeVita for providing all details on the muscle lever arms used in their reduction approach.

Appendix

The muscle groups' lever arms and line of action orientations (L_i^j and $\mathbf{u}^j$ with i = 1, 2, 3 and j = 1, 2, 3) in Eq. (1) are defined as a 10th order polynomial function of the ankle, knee, or hip flexion-extension angle (θ_1, θ_2, or θ_3). They are based on a synthesis of literature data performed by DeVita and Hortobagyi (2001). A 10th order polynomial fitted on centred and scaled data was required to interpolate this synthesis of the literature with an error below 1 mm. Note that according to the ISB convention (Wu et al., 2002), the knee flexion-extension θ_2 is negative.

The lever arm of the gastrocnemii (j = 1) with respect to the ankle (i = 1), L_1^1, is given as a polynomial function of the ankle flexion-extension angle (θ_1) while the lever arm with respect to the knee (i = 2), L_2^1, is given as a polynomial function of the knee flexion-extension angle (θ_2). The lever arm of the quadriceps (j = 2) with respect to the knee (i = 2), L_2^2, is given as a polynomial function of the knee flexion-extension angle (θ_2). The lever arm of the hamstrings (j = 3) with respect to the knee (i = 2), L_2^3, is given as a polynomial function of the knee flexion-extension angle (θ_2) while the lever arm with respect to the hip (i = 3), L_3^3, is given as a polynomial function of the hip flexion-extension angle (θ_3). All polynomial coefficients p, centres c, and scales s are provided in Table A1:

$$L_i^j = \sum_{k=0}^{10} p_k^j \left(\frac{\theta_i - c^j}{s^j}\right)^k \tag{A1}$$

The muscle groups line of action orientations $\boldsymbol{u}^j$ are defined by an angle, α_2^j, with respect to the vertical axis of the shank segment, $\mathbf{Y}_2$. Thus, $\mathbf{u}^j \cdot \mathbf{X}_2 = \sin\left(\alpha_2^j\right)$ and $\mathbf{u}^j \cdot \mathbf{Y}_2 = \cos\left(\alpha_2^j\right)$. The angles α_2^j (j = 1, 2, 3) are given as a polynomial function of the knee flexion-extension angle (θ_2). All polynomial coefficients p, centres c, and scales s are provided in Table A2:

Table A1
Polynomial coefficients p, centres c, and scales s defining the lever arms of the muscles groups with respect to the joints as a function of the joint angle.

			$p_0^j*1e^5$	$p_1^j*1e^5$	$p_2^j*1e^5$	$p_3^j*1e^5$	$p_4^j*1e^5$	$p_5^j*1e^5$	$p_6^j*1e^5$	$p_7^j*1e^5$	$p_8^j*1e^5$	$p_9^j*1e^5$	$p_{10}^j*1e^5$	c^j	s^j
Gastrocnemii	L_1^1(in m)	θ_1 (in °)	−5284.6	94.7	255.5	−49.2	−76.2	1.4	47.1	5.5	−16.1	−1.2	2.0	5	15
	L_2^1(in m)	θ_2 (in °)	−1725.1	−208.8	−174.1	−5.6	121.9	−43.2	−89.7	18.1	30.2	−2.4	−3.7	−45	26
Quadriceps	L_2^2(in m)	θ_2 (in °)	3776.1	583.8	63.5	−421.0	−388.8	230.0	92.4	−118.5	4.1	23.1	−1.2	−45	26
Hamstrings	L_2^3(in m)	θ_2 (in °)	−3346.2	591.6	−273.0	−383.0	869.1	−56.3	−651.2	74.0	204.6	−13.1	−23.5	−45	26
	L_3^3(in m)	θ_3 (in °)	−7449.6	−425.4	1120.2	−523.4	161.4	390.4	−43.9	−119.2	−3.9	13.5	1.5	30	35

With $L_i^j = \sum_{k=0}^{10} p_k^j \left(\frac{\theta_i - c^j}{s^j}\right)^k$.

Table A2
Polynomial coefficients p, centres c, and scales s defining the orientation of the line of action of the muscles groups with respect to the shank segment as a function of the knee joint angle.

			$p_0^j*1e^3$	$p_1^j*1e^3$	$p_2^j*1e^3$	$p_3^j*1e^3$	$p_4^j*1e^3$	$p_5^j*1e^3$	$p_6^j*1e^3$	$p_7^j*1e^3$	$p_8^j*1e^3$	$p_9^j*1e^3$	$p_{10}^j*1e^3$	c^j	s^j
Gastrocnemii	α_2^1 (in °)		3000												
Quadriceps	α_2^2 (in °)	θ_2 (in °)	9924.9	5706.0	−1379.6	928.1	−330.9	404.9	351.0	−316.4	−98.6	48.4	8.9	−45	26
Hamstrings	α_2^3 (in °)	θ_2 (in °)		1000										0	1

With $\alpha_2^j = \sum_{k=0}^{10} p_k^j \left(\frac{\theta_2 - c^j}{s^j}\right)^k$.

$$\alpha_2^j = \sum_{k=0}^{10} p_k^j \left(\frac{\theta_2 - c^j}{s^j}\right)^k \quad \text{(A2)}$$

Note that two muscle groups' lines of action were assumed to have a constant orientation (DeVita and Hortobagyi, 2001; Messier et al., 2011). The gastrocnemii ($j = 1$) are assumed to be 3° from parallel with the shank segment, while the hamstrings ($j = 3$) are assumed to remain parallel to the thigh segment.

References

Barrios, J., Willson, J., 2016. Minimum detectable change in medial tibiofemoral contact force parameters: derivation and application to a load-altering intervention. J. Appl. Biomech. 33, 171–175.

Bowersock, C.D., Willy, R.W., DeVita, P., Willson, J.D., 2017. Reduced step length reduces knee joint contact forces during running following anterior cruciate ligament reconstruction but does not alter inter-limb asymmetry. Clin. Biomech. 43, 79–85.

Damsgaard, M., Rasmussen, J., Christensen, S.T., Surma, E., de Zee, M., 2006. Analysis of musculoskeletal systems in the AnyBody Modeling System. Simul. Model. Pract. Theory 14, 1100–1111.

Delp, S.L., Anderson, F.C., Arnold, A.S., Loan, P., Habib, A., John, C.T., Guendelman, E., Thelen, D.G., 2007. OpenSim: open-source software to create and analyze dynamic simulations of movement. IEEE Trans. Biomed. Eng. 54, 1940–1950.

DeMers, M.S., Pal, S., Delp, S.L., 2014. Changes in tibiofemoral forces due to variations in muscle activity during walking. J. Orthop. Res. 32, 769–776.

DeVita, P., Hortobagyi, T., 2001. Functional knee brace alters predicted knee muscle and joint forces in people with ACL reconstruction during walking. J. Appl. Biomech. 17, 297–311.

Dumas, R., Aissaoui, R., de Guise, J.A., 2004. A 3D generic inverse dynamic method using wrench notation and quaternion algebra. Comput. Methods Biomech. Biomed. Eng. 7, 159–166.

Duprey, S., Cheze, L., Dumas, R., 2010. Influence of joint constraints on lower limb kinematics estimation from skin markers using global optimization. J. Biomech. 43, 2858–2862.

Esculier, J.-F., Willy, R.W., Baggaley, M.W., Meardon, S.A., Willson, J.D., 2017. Sex-specific kinetic and kinematic indicators of medial tibiofemoral force during walking and running. The Knee 24, 1317–1325.

Fregly, B.J., Besier, T.F., Lloyd, D.G., Delp, S.L., Banks, S.A., Pandy, M.G., D'Lima, D.D., 2012. Grand challenge competition to predict in vivo knee loads. J. Orthop. Res. 30, 503–513.

Giroux, M., Moissenet, F., Dumas, R., 2013. EMG-based validation of musculo-skeletal models for gait analysis. Comput. Methods Biomech. Biomed. Eng. 16, 152–154.

Heller, M.O., Bergmann, G., Deuretzbacher, G., Dürselen, L., Pohl, M., Claes, L., Haas, N.P., Duda, G.N., 2001. Musculo-skeletal loading conditions at the hip during walking and stair climbing. J. Biomech. 34, 883–893.

Johnson, F., Scarrow, P., Waugh, W., 1981. Assessments of loads in the knee joint. Med. Biol. Eng. Comput. 19, 237–243.

Kernozek, T., Gheidi, N., Ragan, R., 2017. Comparison of estimates of Achilles tendon loading from inverse dynamics and inverse dynamics-based static optimisation during running. J. Sports Sci. 35, 2073–2079.

Kinney, A.L., Besier, T.F., D'Lima, D.D., Fregly, B.J., 2013. Update on grand challenge competition to predict in vivo knee loads. Journal of Biomechanical Engineering 135. 021012-021012-021014.

Knarr, B.A., Higginson, J.S., 2015. Practical approach to subject-specific estimation of knee joint contact force. J. Biomech. 48, 2897–2902.

Messier, S.P., Legault, C., Loeser, R.F., Van Arsdale, S.J., Davis, C., Ettinger, W.H., DeVita, P., 2011. Does high weight loss in older adults with knee osteoarthritis affect bone-on-bone joint loads and muscle forces during walking? Osteoarth. Cartil. 19, 272–280.

Messier, S.P., Mihalko, S.L., Beavers, D.P., Nicklas, B.J., DeVita, P., Carr, J.J., Hunter, D. J., Williamson, J.D., Bennell, K.L., Guermazi, A., Lyles, M., Loeser, R.F., 2013. Strength Training for Arthritis Trial (START): design and rationale. BMC Musculosk. Disorders 14, 208.

Moissenet, F., Modenese, L., Dumas, R., 2017. Alterations of musculoskeletal models for a more accurate estimation of lower limb joint contact forces during normal gait: a systematic review. J. Biomech. 63, 8–20.

Paul, J.P., 1999. Strength requirements for internal and external prostheses. J. Biomech. 32, 381–393.

Perry, J., Burnfield, J., 2010. Gait Analysis: Normal and Pathological Function. SLACK Incorporated, Thorofare NJ, USA.

Sinclair, J., Bottoms, L., 2019. Gender specific ACL loading patterns during the fencing lunge: implications for ACL injury risk. Sci. Sports 34, e31–e35.

Smidt, G.L., 1973. Biomechanical analysis of knee flexion and extension. J. Biomech. 6, 79–92.

Taylor, W.R., Schütz, P., Bergmann, G., List, R., Postolka, B., Hitz, M., Dymke, J., Damm, P., Duda, G., Gerber, H., Schwachmeyer, V., Hosseini Nasab, S.H., Trepczynski, A., Kutzner, I., 2017. A comprehensive assessment of the musculoskeletal system: the CAMS-Knee data set. J. Biomech. 65, 32–39.

Thelen, D.G., Won Choi, K., Schmitz, A.M., 2014. Co-simulation of neuromuscular dynamics and knee mechanics during human walking. J. Biomech. Eng. 136. 021033–021033 021038.

Trinler, U., Hollands, K., Jones, R., Baker, R., 2018. A systematic review of approaches to modelling lower limb muscle forces during gait: applicability to clinical gait analyses. Gait Post. 61, 353–361.

Willy, R.W., Meardon, S.A., Schmidt, A., Blaylock, N.R., Hadding, S.A., Willson, J.D., 2016. Changes in tibiofemoral contact forces during running in response to in-field gait retraining. J. Sports Sci. 34, 1602–1611.

Winby, C.R., Lloyd, D.G., Besier, T.F., Kirk, T.B., 2009. Muscle and external load contribution to knee joint contact loads during normal gait. J. Biomech. 42, 2294–2300.

Wu, G., Siegler, S., Allard, P., Kirtley, C., Leardini, A., Rosenbaum, D., Whittle, M., D'Lima, D.D., Cristofolini, L., Witte, H., Schmid, O., Stokes, I., 2002. ISB recommendation on definitions of joint coordinate system of various joints for the reporting of human joint motion—part I: ankle, hip, and spine. J. Biomech. 35, 543–548.